THERMAL-HYDRAULIC STUDY OF THE PRIMARY HEAT TRANSPORT SYSTEM OF THE DEMO DIVERTOR CASSETTE BODY

F. M. Castrovinci
Department of Engineering, University of Palermo
Viale delle Scienze, Ed. 6, 90128 Palermo, Italy
francescamaria.castrovinci@unipa.it

L. Barucca
Ansaldo Nucleare
Via N. Lorenzi 8, 16152 Genova, Italy

S. Basile
Department of Engineering, University of Palermo
Viale delle Scienze, Ed. 6, 90128 Palermo, Italy

R. Burlon
Department of Engineering, University of Palermo
Viale delle Scienze, Ed. 6, 90128 Palermo, Italy

P. Chiovaro
Department of Engineering, University of Palermo
Viale delle Scienze, Ed. 6, 90128 Palermo, Italy

P. A. Di Maio
Department of Engineering, University of Palermo
Viale delle Scienze, Ed. 6, 90128 Palermo, Italy

M. Giardina
Department of Engineering, University of Palermo
Viale delle Scienze, Ed. 6, 90128 Palermo, Italy

A. Quartararo
Department of Engineering, University of Palermo
Viale delle Scienze, Ed. 6, 90128 Palermo, Italy

A. Tincani
ENEA Bologna Research Centre
Via Martiri di Monte Sole 4, 40129 Bologna, Italy

E. Vallone
Department of Engineering, University of Palermo
Viale delle Scienze, Ed. 6, 90128 Palermo, Italy

April 28, 2023

ABSTRACT

The EU-DEMO reactor is supposed to undergo a pulsed duty cycle under normal conditions, which might challenge the qualified lifetime of the main equipment inducing undue thermal and mechanical cycling loads. Moreover, during power operation it is not possible to exclude the occurrence plasma overpower transients that might jeopardize the structural integrity of the plasma-facing components. In this context, the University of Palermo in cooperation with ENEA has launched a research campaign within the framework of the EUROfusion action to investigate the thermal-hydraulic behaviour of the Primary Heat Transport System (PHTS) of the EU-DEMO Divertor (DIV) Cassette Body (CB) during the typical DEMO duty cycle. The study was primarily intended to start the definition of the strategies to be followed to minimize thermal fluctuations due to the pulsed operation. In particular, the attention has been focussed on the assessment of the DIV CB PHTS temperature behaviour during the pulse-dwell transition so to check the potential effectiveness of a direct coolant temperature control by properly tuning the feedwater mass flow rate. The activity has been led following a computational approach based on the adoption of the TRACE thermal-hydraulic system code. Models, assumptions, and outcomes of the analyses are herewith reported and critically discussed.

1 Introduction

DEMO is going to be the first fusion device that will produce electricity and, hence, it shall be provided with a proper Balance of Plant (BoP) system that must meet many of those design criteria and safety requirements characterising the most common nuclear power station. Nevertheless, contrary to common Nuclear Power Plants (NPPs), DEMO is supposed to undergo a pulsed duty cycle during normal operative conditions. Consequently, it will be subjected to oscillating loads that might challenge the qualified lifetime of the main BoP equipment inducing undue thermal and mechanical cycling.

Although it is rather impossible to prevent the occurrence of such cycling in the components of the Primary Heat Transport Systems (PHTSs), several strategies are being considered to cope with the potential negative effects of the pulsed operations on the main components of the Power Conversion System (PCS), such as turbine and steam generators. In this direction, the reference configuration for the BoP of a DEMO reactor equipped with a Water Cooled Lithium Lead Breeding Blanket (WCLL BB) is based on a Direct Coupling Design (DCD) equipped with a small Energy Storage System (ESS) [1]. In order to maintain the connection to the electrical grid with a minimum production of the electricity (enough for the PHTSs and BoP auxiliaries) while limiting thermal stresses on the main PCS components, this option encompasses a small ESS operated with molten salt (HITEC), capable of feeding the steam turbine during dwell with a steam flow rate of about 10% of the nominal steam flow rate. The Once Through Steam Generators (OTSGs) of Breeding Zone and First Wall PHTSs are directly connected with the steam turbine of the PCS while the thermal power removed from Divertor (DIV) and Vacuum Vessel (VV) is used to pre-heat the PCS feed-water, together with the most common regenerative heaters fed by the steam extraction lines.

During the DEMO pre-conceptual design phase, the main BoP components have been preliminarily designed considering a fixed, steady-state working point. However, during its lifetime, the reactor will experience several operational (and, maybe, accidental) transients that will bring the main thermal-hydraulic parameters of the system in different conditions than the reference design ones. It is hence necessary to study the global behaviour of the system to know its response under these transient scenarios.

In this context, the University of Palermo has started a research campaign to investigate the thermal-hydraulic behaviour of the PHTS of the EU-DEMO Divertor Cassette Body (CB) under transient conditions. The thermal-hydraulic behaviour of the cooling circuit during the typical DEMO duty cycle has been investigated to understand the response of the system during nominal operational transients and begin the definition of the strategies to be followed to minimize the thermal fluctuations due to the power variations. The activity has been led following a computational approach based on the adoption of the TRACE thermal-hydraulic system code [2]. Models, assumptions, and outcomes of the analyses are herewith reported and critically discussed.

2 The DEMO Divertor Cassette Body PHTS

The divertor is a key in-vessel component in a nuclear fusion reactor, being responsible for power exhaust and impurity removal via guided plasma exhaust. The viability of fusion power generation heavily depends on the heat loads that can be tolerated by the divertor under normal and off-normal operation. Therefore, particular attention must be paid to the thermal-hydraulic design of its cooling system, to ensure safe and reliable operations.

The latest DEMO Divertor is articulated in 48 cassettes [3], each composed of a Cassette Body (CB), equipped with a Liner and two Reflector Plates (RPs) which are hydraulically and mechanically connected to a supporting structure (fig. 1). Moreover, each CB supports two Plasma Facing Components (PFCs), namely an Inner Vertical Target and an Outer Vertical Target.

Due to the different heat loads and several structural requirements the CBs and the PFCs have to withstand [4], they must be cooled by two separate circuits, fed by water coolant at different T/H conditions. As a matter of fact, the heat flux impacting the CB Liner is mainly due to radiation and hence, the main source of power deposited comes from nuclear heating. On the other hand, the two PFCs have to sustain the nuclear power deposited by neutrons and gammas, as well as the high heat fluxes due to irradiation and particles arising from plasma (up to 20 MW/m^2), much higher than that experienced by CBs. The reference CB coolant operating conditions assumed for the present activity are summarized in table 1.

The CB allows the water coolant at 180 °C and 35 bar coming from inlet manifold, routed through the lower port, to enter from the outboard side and flow in the CB top part up to the Liner and the RPs inlets that are fed in parallel. Once the coolant has been routed through these sub-circuits, removing the deposited power, it continues its path toward the inboard side of the CB. From this region, the water goes downward and, after flowing through the bottom part of the CB, it reaches the outlet manifold that routes the coolant outside the VV through the lower port.

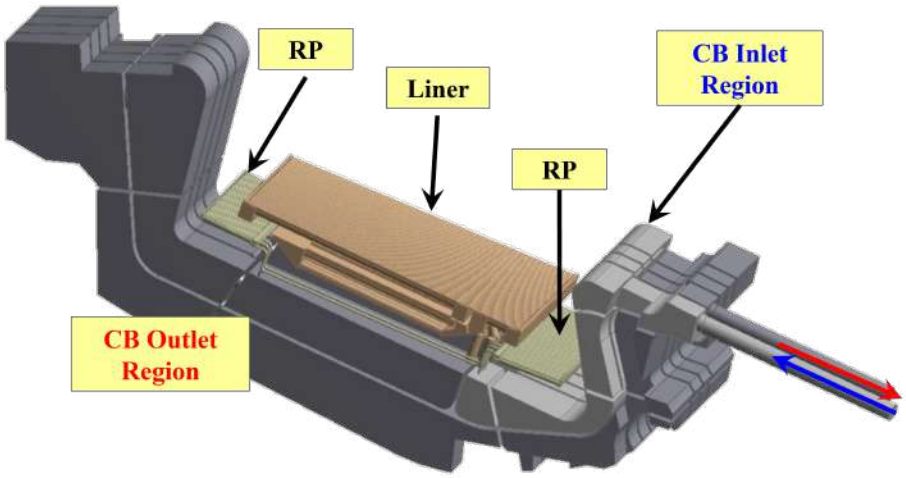

Figure 1: The DEMO Divertor Cassette Body.

Table 1: Summary of CB reference operating conditions.

Coolant [-]	Water
Divertor cassettes [-]	48
Deposited power [MW]	115.2
Inlet pressure [MPa]	3.50
Mass Flow Rate [kg/s]	17.94
Inlet temperature [°C]	180.0
Outlet temperature [°C]	210.0

The material selected for the CB structure is Eurofer [5], while a layer of Tungsten [6] covers the plasma-facing surfaces of Liner and RPs.

The main function of the DIV CB PHTS (fig. 2) is to extract thermal power from the DIV CB and transfer it to the PCS through Heat eXchangers (HXs) that act as PCS feed-water pre-heaters as well as to provide containment boundary to the primary coolant [7]. In addition, it has also the function of limiting the air and secondary coolant in-leakage.

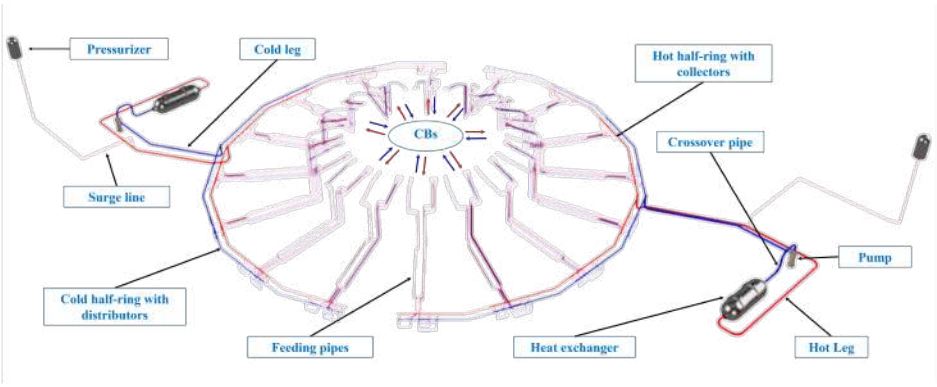

Figure 2: The DEMO DIV CB PHTS.

The DIV CB PHTS is subdivided into two independent cooling loops, each one feeding eight DIV sectors for a total of 24 DIV CBs. Each cooling loop consists of in-vessel circuits, a HX, a pressurizer (PRZ), a main coolant pump and connecting pipes. Hot (cold) manifolds of each circuit are arranged to form a hot (cold) half-ring, which collects (distributes) the coolant among the feeding pipes. The PHTS piping (per each cooling loop) foresees hot leg, cold leg, collector, distributor and six feeding pipes per each sector (3 pipes to retrieve hot water from each sector and 3 to feed them with cold water).

Main coolant pumps deliver, under nominal conditions and during plasma flat-top, cold coolant at 180 °C to the DIV CB PHTS via the cold pipework. Downstream the pump, water flows into the main cold leg, then it reaches the cold half-ring where it is distributed through the manifolds (distributors) among the cold feeding pipes toward the CBs. Entering the In-Vessel components, the coolant removes the power from the structures of the Cassettes and exits those elements at about 210 °C and higher enthalpy. Once the water leaves the different CBs, it follows the whole hot feeding pipe length up to the hot manifolds (collectors) in the hot half-ring where it is collected and redirected into the hot legs to reach the HX. Here the primary coolant exchanges the carried thermal power with the feedwater on the secondary side. Finally, water exits the exchanger and flows through the crossover pipe up to the pump suction inlet, where it finishes its closed loop and is ready to start the next thermal cycle.

3 Thermal-hydraulic analysis campaign

During 2021, the University of Palermo has started a research campaign to investigate the thermal-hydraulic behaviour of the DIV CB PHTS under steady-state and transient conditions.

The research activity has been initially centred on the assessment of the spatial distribution of coolant mass flow rates and pressure drops along the DIV CB PHTS under hypothetical steady-state conditions corresponding to a pulse period of the DEMO duty cycle to check that an adequate cooling is ensured to all the CBs.

Afterwards, the thermal-hydraulic behaviour of the DIV CB PHTS during the typical DEMO duty cycle has been investigated mainly in order to start the definition of the strategies to be followed to minimize the thermal fluctuations due to the pulsed operation. In particular, the attention has been especially focussed on the assessment of the DIV CB PHTS temperature behaviour during the pulse-dwell transition so to check the potential effectiveness of a direct coolant temperature control. To this purpose, the effectiveness of several regulation strategies of the feedwater mass flow rate has been assessed.

The activity has been carried out following a theoretical-computational approach based on the finite volume method and adopting a suitable release of the TRACE thermal-hydraulic system code family [2].

3.1 Model setup

Since the DIV CB PHTS is made of two equal and separate circuits [7], a single coolant loop has been simulated. According to the requirements of the TRACE system code, attention has been focused on the development of a realistic finite volume model that might be able to capture all the main thermal-hydraulic features characterizing both in-vessel and ex-vessel components.

Actually, the computational model consists of four main sub-models:

- the geometrical sub-model, reproducing in a quasi-2D approximation the layout of the cooling circuit;
- the constitutive sub-model, provided by the system code to describe the thermo-dynamic behaviour of the water circulating inside the cooling system;
- the hydraulic sub-model, intended to simulate the fluid flow along the cooling system;
- the thermal sub-model articulated in different sub-patterns aimed at realistically reproducing the heat transfer phenomena that take place along the cooling system.

Each one of the TRACE sub-models of the WCLL BB PHTS will be described in detail in this paragraph. Additionally, a comprehensive overview of the control systems adopted to regulate the main PHTS thermal-hydraulic parameters will be given.

3.2 Geometrical sub-model

A quasi-2D geometrical model has been set up, which realistically simulates the flow domain of the investigated cooling circuit. The flow domain discretization has been performed saving the volume of each component so that the overall coolant amount could be accurately modelled. Moreover, sub-volumes have been properly oriented in space to reproduce their relative positions and heights. Therefore, both distributed pressure drops and gravitational effects have been properly modelled, at least as far as geometrical parameters involved in their evaluation are concerned. Furthermore, the model nodalization has been developed to realistically predict the overall thermal-hydraulic behaviour of the selected loop while demanding admissible computing time.

In fig. 3 the TRACE model of the entire PHTS loop is reported while fig. 4 shows a detailed view of the nodalization of the DIV CB.

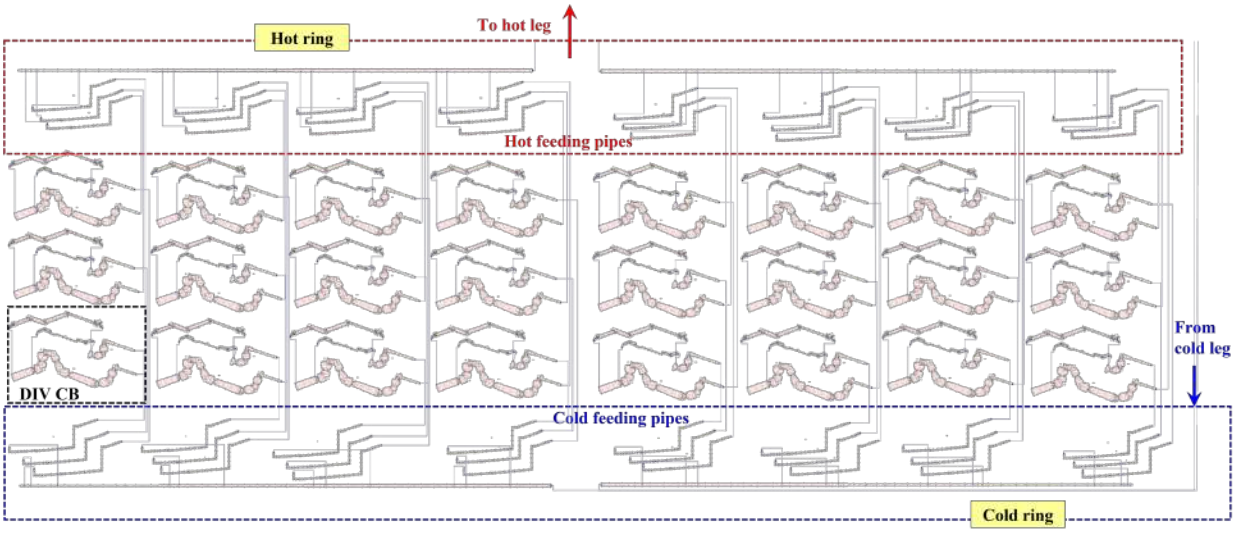

Figure 3: Finite volume model of the DIV CB PHTS.

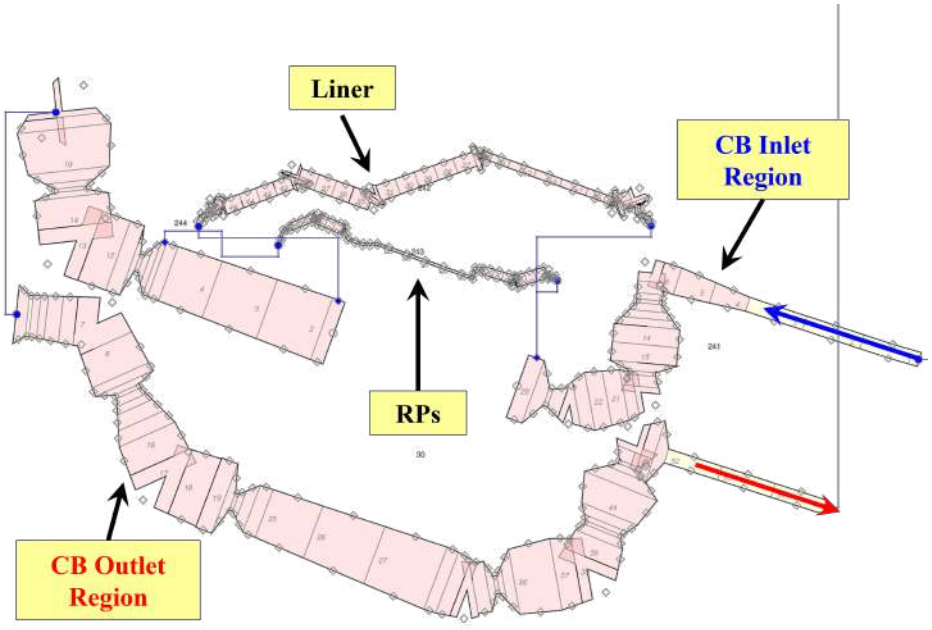

Figure 4: Finite volume model of the DIV CB.

In this regard, it is worth to highlight that each DIV CB has been modelled by using four pipes representing the regions identified in fig. 1, namely CB inlet region, liner, RPs, and CB outlet region.

According to the design described in [8], the HX section has been modelled as being composed of two identical HX units, as shown in fig. 5. Concerning the PCS, its modeling has been limited to the HX secondary side. Upstream and downstream equipment have been simulated by means of a fill and a break component, respectively, which allows reproducing the feedwater flow manoeuvres vs load to be envisaged by the PCS designers.

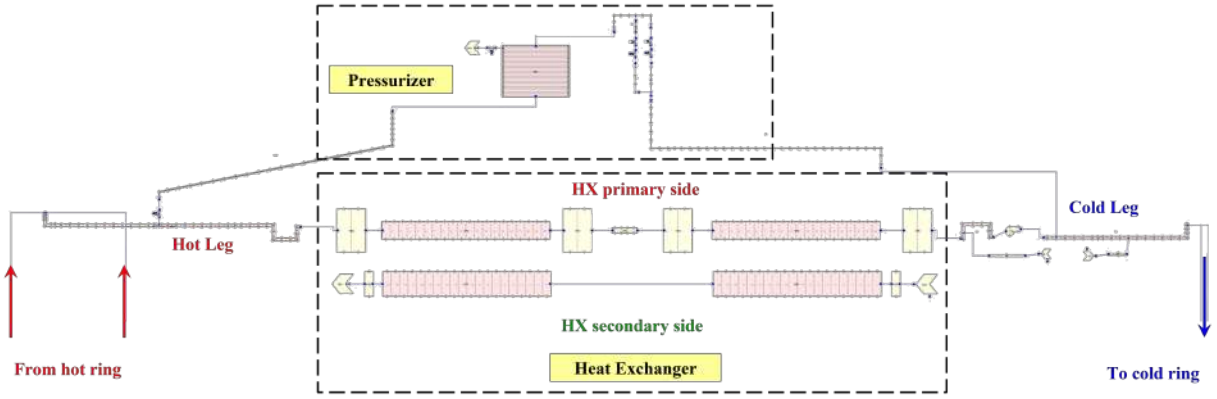

Figure 5: TRACE model of pressurizer and HX.

The pressurizer is modelled using a pipe component and it is connected to the hot leg and to the cold leg through the surge line and the spray line, respectively. The former one is connected to the bottom of the pressurizer while the latter one connects the cold leg downstream the delivery of the pump to the top head of the pressurizer. The spray line branches in an emergency spray and a continuous spray. Each branch is equipped with a control valve and a check valve. The control valve on the emergency spray line is normally closed while the opening of the valve on the continuous spray line has been preliminarily set to balance the pressurizer heaters power during normal operations.

Furthermore, it may be noticed from fig. 5 that the connections to the CVCS, i.e. the makeup/charging line and the letdown line, have been included. The regulation of makeup and letdown mass flow rates provides control of the pressurizer level and, hence, of the total coolant inventory.

3.3 Constitutive sub-model

Constitutive models provided by the TRACE system code have been adopted to describe the thermo-dynamic behaviour of water coolant circulating inside the DIV CB PHTS cooling system. The model is based on proper libraries describing the dependence of water thermo-physical properties on pressure and temperature. Different materials have been considered to realistically model the thermal behaviour of the different ex-vessel and in-vessel structural components.

As far as the Cassette Body is concerned, thermophysical properties of both EUROFER [5] and Tungsten [6] have been implemented in the code as a function of temperature. Concerning the PHTS pipe network, the built-in material Stainless 316 has been adopted while, for the Microtherm® SLATTED insulation [7], a user-defined material has been introduced in the model, whose thermo-physical properties have been drawn from [9]. Regarding the pressurizer structure, the SA-508 Gr.3 Class 2 low-alloy steel has been selected and implemented with its thermophysical properties [10] in the code, while for both proportional and backup heaters the material constantan/nichrome has been selected from the TRACE code built-in library. Finally, regarding the HX, only the tube bundles structures have been simulated and the material defined is Inconel 690 [10].

3.4 Hydraulic sub-model

The hydraulic model has been set up to properly simulate water single-phase and/or two-phase flow inside the investigated cooling circuit. Both frictional losses Δp_{fr} and local resistance Δp_{loc} in the pipeline are considered in the model. Frictional losses depend on the Darcy friction factor which is evaluated by the TRACE code according to the Churchill formula [11]. It depends on the Reynolds number (Re) [12] and on the equivalent wall roughness that, for the present activity, has been assumed equal to 15 μm for the in-vessel components [4] and 50 μm for the ex-vessel ones [7]. On the other hand, the concentrated hydraulic resistances occurring within the flow domain have been modelled by considering their possible functional dependence on the flow velocity field through the concentrated loss factor

(K_{loc}), whose values have been derived in different ways depending on whether the DIV CBs or the ex-vessel PHTS are concerned.

To capture the effect of the complex 3D layout of the DIV CBs on their hydraulic behaviour, a specific approach has been adopted [13], integrating the TRACE system code with the ANSYS CFX [14] 3D CFD code, to give as an input to the TRACE code the functional dependence of the circuit effective concentrated loss coefficient on the Reynolds number.

Concerning the ex-vessel PHTS, the concentrated hydraulic loss coefficients have been drawn from the well-known Idelchik's handbook [15], according to the specific geometrical configurations and flow conditions.

Concerning the pump component, since a detailed design of the main coolant pump of the DIV CB PHTS is not yet available because the DEMO project and, hence, its PHTSs are still at a pre-conceptual level, the built-in Westinghouse characteristic curves have been preliminarily adopted along with the main design parameters suggested in [16].

3.5 Thermal sub-model

In order to accurately model the heat transfer phenomena within the DIV CB PHTS, the discretization of the solid domain has been performed saving volumes and heat transfer areas of each structural component, wherever possible, and adopting properly selected heat transfer models, whenever needed.

Particular attention has been paid to the modelling of the solid domain of the Cassette Body. In particular, as far as Liner and RPs are concerned, their solid structures have been simulated by means of two different slab-type heat structure components; one of them is relevant to the plasma-facing region, including the Tungsten and the EUROFER layers, while the other one is meant to reproduce the remaining part which is in EUROFER. The RPs plasma-facing region has been further divided in two heat structures, one of them being connected to the inner RP while the other one to the outer RP.

The plasma-facing heat structures of Liner ad RPs have been modelled considering the 2 mm-thick tungsten layer while the EUROFER layer thickness has been assumed equal to the minimum distance between the tungsten layer and the plasma-facing channels, i.e. 2 mm. The heat structure surface has been set equal to the actual plasma-facing surface for both Liner ad RPs.

Concerning the remaining part of the Liner and RPs solid domain, the heat structure surface has been derived from the overall area of the fluid-solid interface while an equivalent thickness has been determined so to save the volume of the solid structures and, hence, their thermal inertia.

On the other hand, as far as the cassette body is concerned, two different cooling regions may be identified, namely the upper CB region, where water flows from the inlet manifold to the inboard part of the CB, and the lower CB region, where fluid flows from the inboard side to the outlet manifold. Due to the peculiar coolant flow arrangement within the CB cooling circuit, the cold stream crossing the upper CB region exchanges thermal power through a metal rib with the hot fluid passing through the lower CB region in the opposite direction. In order to take into account the heat transfer across this interface, a single heat structure connecting the two CB regions has been defined. In particular, the heat transfer area has been assumed equal to the average fluid-solid interface area of the two CB regions while an equivalent thickness has been determined so to save the volume of the metallic structures and, hence, their thermal inertia.

Concerning the heat loads, uniform surface heat fluxes have been considered as external boundary conditions for both Liner and RPs plasma-facing surfaces, while volumetric heat loads have been modelled via the power component, which provides the implementation of the generated or deposited power inside structural materials, and the fluid power component for the deposited power in fluids. In this respect, in order to be consistent with the latest design of the DIV CB PHTS [7], the thermal loads reported in [4] have been scaled down so to match the reference thermal power adopted by WPBoP designers (i.e. 115.2 MW).

The scaled heat fluxes used as input for the TRACE model of the DIV CB PHTS are 0.575 MW/m^2 and 0.115 MW/m^2 for Liner and RPs, respectively, while the scaled volumetric heat loads are reported in table 2.

Under normal operating conditions, the heat loads vary in time according to the DEMO duty cycle reported in fig. 6. It comprises two main phases where the reactor power ranges from 100% to a minimum of about 1÷2% of its nominal value, mainly due to the residual heat into the tokamak structures. The two phases are called Pulse and Dwell time and last 2 hours and about 10 minutes, respectively. The transition from one phase to the other is made by two transitional phases, namely plasma ramp-up and ramp-down, that last about 100-200 seconds each.

For the purpose of the present calculation, ramps are assumed to last 200 s and heat loads are assumed to vary linearly during these periods. Specifically, heat flux on the plasma-facing surfaces is supposed to range from its nominal value

Table 2: Volumetric heat loads.

Component	Power per Cassette [MW]
Liner Armour	0.048
Liner Structure	0.450
Liner Coolant	0.213
RPs Armour	0.014
RPs Structure	0.052
RPs Coolant	0.017
CB Structure	0.449
CB Coolant	0.216
TOTAL	1.460

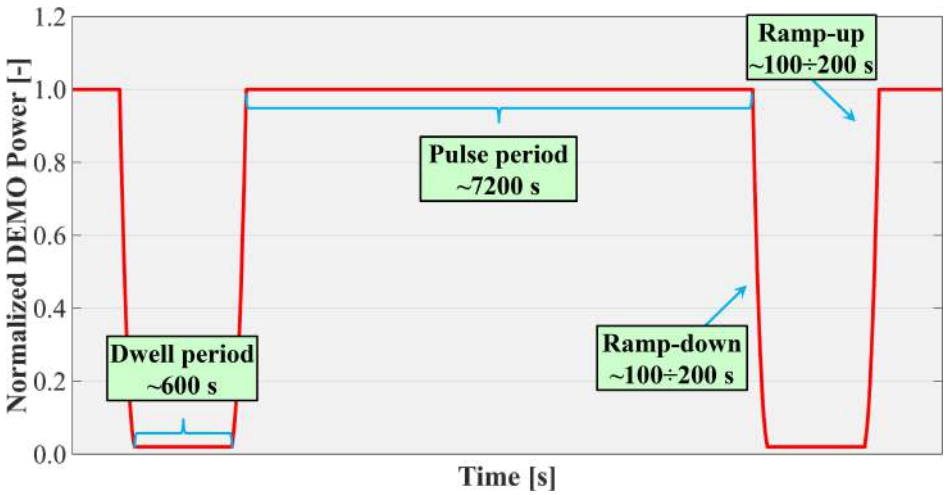

Figure 6: Duty cycle of DEMO pulsed operation.

during the pulse period to zero during the dwell time. The same trend has been adopted for the nuclear power deposited into the coolant within the CBs. On the other hand, the nuclear power deposited into the CB structures varies from its nominal value during the pulse period to a value corresponding to the residual decay heat at shutdown during the dwell time [17].

Concerning the ex-vessel PHTS pipe network, heat structures made up of two layers have been implemented so to consider the AISI 316LN steel and the insulation. Furthermore, the heat exchange with the environment has been properly reproduced by connecting each heat structure to a large hydraulic volume simulating the tokamak building and imposing the pertaining Heat Transfer Coefficient (HTC) calculated a-priori, adopting the Churchill&Chu correlation [18].

Pressurizer heaters are located vertically in the lower hemisphere of the pressurizer to heat the contained water to saturation and produce steam for pressure control. The heaters are divided into a proportional heater bank and a backup heater bank. The heat output from the proportional heaters varies in proportion to the difference between the measured pressure (in the upper head) and the set point pressure while the backup heaters operate by on-off control, providing heat for large changes in plant condition. The pressurizer heaters have been implemented in TRACE system code as two cylindrical heat structures, one for the proportional heaters and one for the backup heaters. In this case, to implement the contact with the pressurizer fluid, the lower hydraulic volumes of the pressurizer have been used as an external boundary condition for heaters heat structures. Both heat structures have been associated with their relevant power components, simulating their power capacity that has been set equal to 88 kW and 107 kW for the proportional heaters and the backup heaters, respectively.

The other ex-vessel component that has been considered in the TRACE thermal sub-model is the heat exchanger. The HX type considered is the “tube and shell” type with counter-current straight tubes, composed of two shells in series [8]. As far as the HX primary side is concerned, it has been simulated using two equivalent pipes in series with their relatives HX heads (implemented as separated pipes). The two tube banks are equipped with a single cylindrical heat structure in Inconel 690. The BCs implemented for this heat structure are the contact with the tube bundles hydraulic volumes as internal BC and the contact with the shell hydraulic volumes in counter current as external BC. Moreover, to

include the effect of the skin thermal resistance localized on the tube walls due to deposits and rust, a thin layer of a fake material that simulates the fouling layer has been introduced in the model. In particular, the thermal resistance given by the equivalent fouling layer amounts to $1.76\mathrm{e}{-4}$ $\mathrm{m}^2\mathrm{K/W}$ according to [19] and [20].

Another thermal contribute that should be considered is the pump frictional heating. The pump model provided by the TRACE system code can account for energy deposited to the fluid through irreversible friction losses in the pump impellers by adding source terms to the liquid and vapour energy equations. It should be noted that for pumped flow around a closed loop, in general, the work done on the fluid by the pump will appear as an energy source that uprises in form of frictional losses, causing a fluid enthalpy increase. This is currently not simulated in TRACE [2]. This contribution has been introduced directly in the pump model via a fluid power component linked to a control system that multiplies the pump frictional torque and the pump velocity for the pump efficiency.

3.6 Control systems

The architecture of the control systems developed for the DIV CB PHTS has been inspired by Pressurized Water Reactors (PWRs) regulation strategy [21, 22, 23]. In particular, three main control systems have been included in the model and namely:

- the pressurizer pressure control system;
- the pressurizer level control system;
- the feedwater flow control system.

The pressurizer pressure control system controls the pressure of the PHTS at a fixed setpoint. The system consists of a combination of electric heater banks, spray valves, and relief valves actuated at the proper times by a Proportional-Integral (PI) pressure controller.

The pressurizer heaters are divided into two groups, consisting of one bank of variable heaters, and several banks of backup on-off heaters. The variable heaters are operated by directly controlling their heat output over a fixed pressure range. During steady-state operation, the proportional heaters compensate for the continuous bypass spray flow and for heat losses from the pressurizer to ambient as well as for minor pressure fluctuations. If the pressure in the PRZ decreases from the desired pressure of 31.5 bar, the master controller increases the output of the proportional heaters. If the pressure continues to decrease, all banks of backup heaters are turned on. As the heaters add energy to the water in the pressurizer, more water flashes to steam, thereby increasing the pressure to the desired setpoint. As the pressure in the PRZ increases above its normal setpoint, the master controller decreases the output of the proportional heaters. If the pressure continues to increase, the master controller output modulates the spray valves open. Opening the spray valves allows reactor coolant to flow from the PHTS cold leg through the spray nozzle into the pressurizer. The relatively cool water spraying into the steam space of the pressurizer condenses some of the steam, which in turn lowers pressurizer pressure. Heater response is shown in fig. 7 for both variable heater, and backup heaters while fig. 8 shows the spray valve area fraction as a function of pressure error.

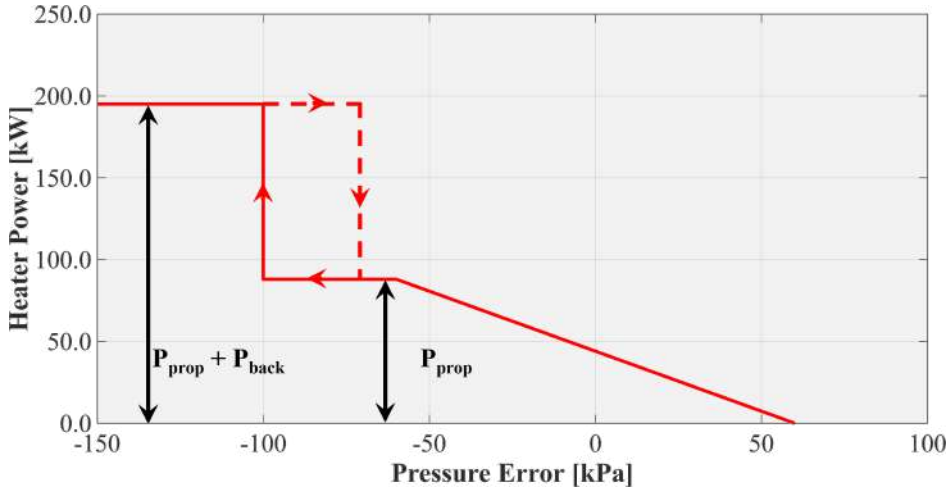

Figure 7: Heater response as a function of pressure error.

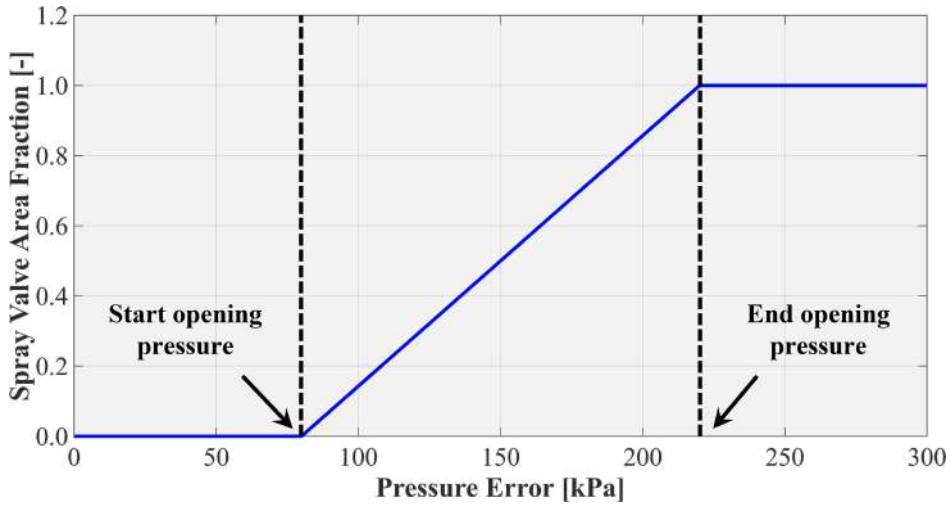

Figure 8: Emergency spray area fraction as a function of pressure error.

The pressure from the PRZ top head is compared to a pressure setpoint (normally 31.5 bar). The resulting pressure error is the input to the master pressure controller, which is a PI controller. The integral action of the controller causes the controller output to vary with the duration of the pressure error and thus serves to return pressurizer pressure to setpoint. The output from the master pressure controller provides input signals to the controllers for the proportional heaters and the spray valves. The master controller also provides inputs to the bistable that energizes the backup heaters.

The power output of the proportional heaters varies linearly between the nominal setpoints of the master pressure controller being 30.9 bar (proportional heaters fully energized) and 32.1 bar (proportional heaters de-energized). The backup heater banks have an off-on-automatic control switch which is dependent on the output of the master controller. The nominal setpoints are 30.5 bar (1.0 bar below setpoint) for the heaters to energize and 30.7 bar (0.8 bar below setpoint) for the heaters to de-energize. The amount of modulation of each spray valve is dependent on the output of the master controller. The nominal setpoints (corresponding to the proportional output of the controller only) are 32.3 bar (0.8 bar above setpoint) for spray valves to start opening and 33.7 bar (2.2 bar above setpoint) for spray valves to be fully open. The amount of valve opening varies linearly between the full-closed and full-open setpoints.

For very large pressure transients, spring loaded safety valves are provided on the pressurizer as a final means of protecting the integrity of the reactor coolant system. The pressure relief valve operation is expressed by an "on/off" control action.

The pressurizer level control system functions to maintain the proper water inventory in the reactor coolant system by controlling the balance between water leaving and entering the system. In reactors, the level in the pressurizer is determined by measuring the difference in pressure between an external column of water of a known height (reference leg) and a variable column of unknown height inside the pressurizer (variable leg). The differential pressure between these two columns of water is converted into a pressurizer level signal. The difference between the actual pressurizer level and the programmed reference level signal is supplied to the master pressurizer level controller. If an error signal exists, this PI controller varies the chemical and volume control system charging flow. The same level signal which is compared to the reference level in the level controller is also sent to a trip which provides a low-level interlock at $\approx 27\%$ level in the pressurizer. This interlock turns off all pressurizer heaters so to protect them from being damaged if operated in a steam environment.

When the plant is operating and the power in the reactor is changed, the average temperature of the reactor coolant system is programmed to change. This change in temperature causes a corresponding change in the level of the PRZ. To reduce the effect on the charging system, the target level in the PRZ is programmed as a function of average temperature, so that it follows the natural expansion characteristics of the reactor coolant. However, a rapid transient causes an increase or decrease in the water level of the PRZ and a corresponding response by charging flow. For this reason, both minimum and maximum level limitations are placed on the level program. These latter have been derived from the volume changes that occur in the PHTS in case it is cooled down to the PHTS minimum temperature under normal operating conditions, i.e. $\approx 180^{\circ}C$, and in case it is heated up to the PHTS maximum temperature under normal operating conditions, i.e. $\approx 210^{\circ}C$, respectively. Fig. 9 shows the pressurizer level program as a function of PHTS average temperature.

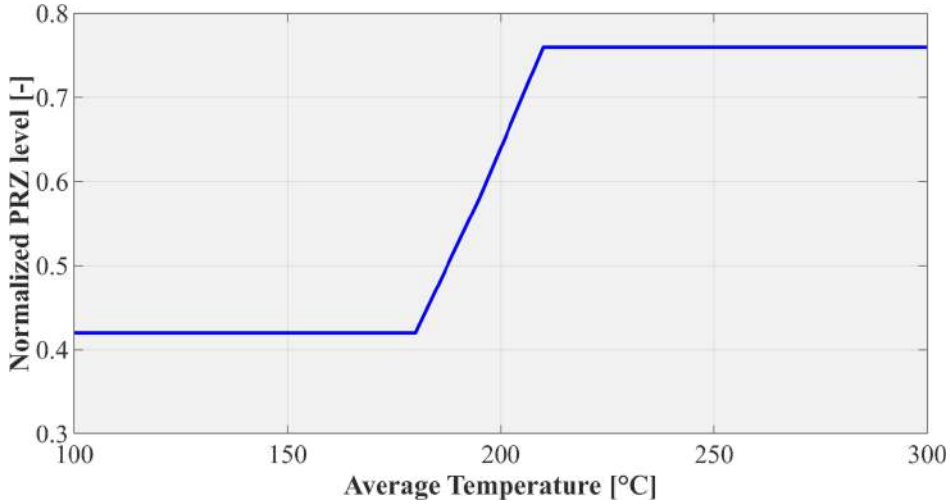

Figure 9: Pressurizer level program.

The feedwater flow control system regulates the mass flow rate flowing through the secondary side of the HX aiming at limiting coolant temperature variations within the PHTS. The feedwater mass flow rate G_{fw} is given by the sum of two contribution. The first one is a time profile defined by the user *G(t)* whose trend is connected to the anticipated load variations, i.e. the ones that may occur during the pulse-dwell transition (fig. 10). The other one is given by a PI (ΔG_{PI}) or a PID (Proportional-Integral-Differential) controller (with the addition of the differential term ΔG_D) whose output is dependent on the difference ΔT between the actual PHTS average temperature and its target value, i.e. 195$°C$. The following equation describes the regulation program for the feedwater mass flow rate.

$$G_{fw} = W_t G(t) + W_{PI} \Delta G_{PI}(t) + W_D \Delta G_D(t) \tag{1}$$

The G(t) contribution is defined by the following time profile reported in fig. 10.

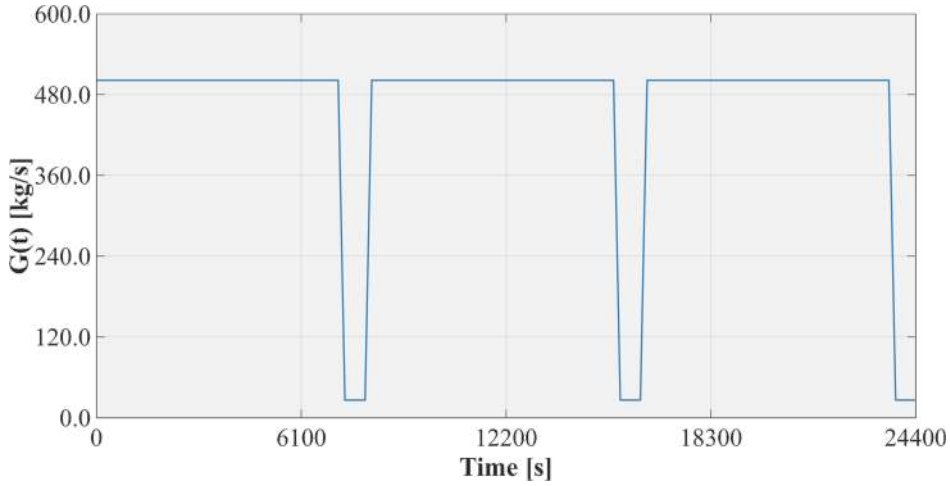

Figure 10: User-defined contribution *G(t)* to feedwater mass flow rate control system.

The PI/PID controller contributions can be expressed by the following eqs. (2) and (3), where K_P, K_I and K_D are the tuning parameters, called, respectively, proportional gain, integral gain and derivative gain.

$$\Delta G_{PI}(t) = K_P \Delta T + K_I \int \Delta T \, dt \tag{2}$$

$$\Delta G_D(t) = K_D \frac{d\Delta T}{dt} \tag{3}$$

By varying the weight coefficients W_i of eq. (1) between 0 and 1, several regulation strategies have been investigated and reported in detail in the next chapter.

4 Preliminary steady-state analysis

The study was primarily intended to start the definition of the strategies to be followed to minimize thermal fluctuations due to the pulsed operation. Nonetheless, the research activity has been initially devoted to the assessment of the spatial distribution of coolant mass flow rates and pressure drops along the DIV CB PHTS during a pulse period of the DEMO duty cycle to check that an adequate cooling is ensured to all the CBs.

Selected results are reported in table 3 and figs. 11 and 12. In particular, table 3 shows a summary of the main thermal-hydraulic parameters during the pulse period compared with analytical calculations that have been performed following the same approach adopted in [7]. Furthermore, fig. 11 shows the coolant Mass Flow Rate (MFR) distribution among the 12 cassettes of the right half of a DIV CB PHTS loop, being representative of all the 24 cooling paths. Divertor CBs MFRs are compared to the nominal MFR with 10% error bars and CBs are numbered starting from the most distant from the legs connection. On the other hand, fig. 12 reports the pressure distribution along the cooling paths relevant to the central CBs of the right half of a DIV CB PHTS loop. Static pressures have been normalized with respect to the CBs nominal inlet pressure (i.e. 3.5 MPa).

Table 3: Steady-state results comparison.

	Design	**TRACE**	ϵ[%]
Loop power [MW]	58.21	57.90	-0.54
Loop MFR [kg/s]	430.62	430.76	0.03
$T_{Cold\ Leg}$ [°C]	180.00	180.04	0.02
$T_{Hot\ Leg}$ [°C]	210.00	209.96	-0.02
p_{PRZ} [MPa]	3.15	3.15	0.00
PRZ level [m]	1.24	1.24	0.01
p_{FW} [MPa]	8.21	8.21	0.00
FW MFR [kg/s]	523.59	501.30	-4.26
$T_{FW\ Inlet}$ [°C]	176.30	176.30	0.00
$T_{FW\ Outlet}$ [°C]	201.50	202.48	0.48

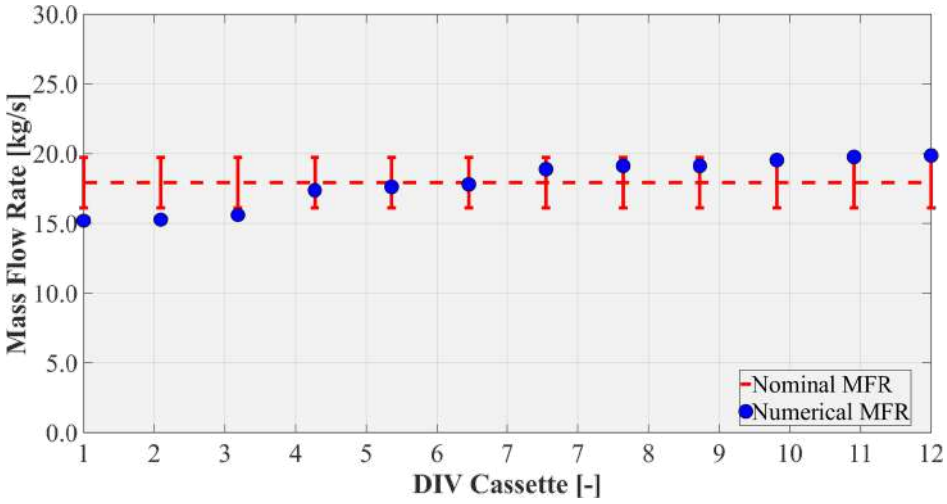

Figure 11: Mass flow rate distribution among DIV CBs.

From the analysis of the results, it may be argued that the main thermal-hydraulic parameters calculated by the TRACE code are very close to analytical results. The maximum deviation has been predicted for the Feed Water (FW) mass flow rate and amounts to 4% of its nominal value.

Looking at fig. 11, a uniform coolant MFR distribution has been predicted with maximum deviation being lower than 15%).

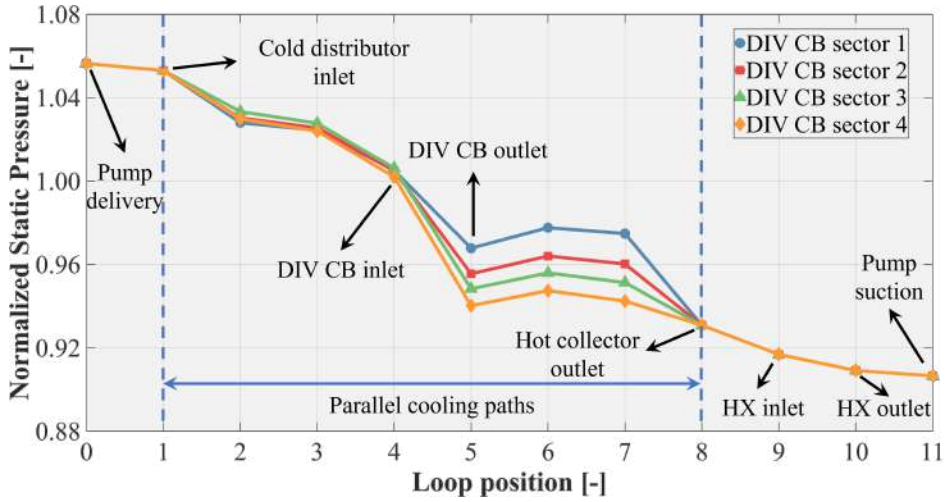

Figure 12: Normalized static pressure distribution for the right side half-ring.

Fig. 12 shows that the predicted pressure distribution correctly reproduces the preliminarily calculated analytical results. The predicted overall pressure drop amounts to 0.53 MPa, being mainly concentrated within the in-vessel component.

5 Transient analyses

In a second phase of the study, the thermal-hydraulic behaviour of the DIV CB PHTS during the typical DEMO duty cycle has been investigated. The study was primarily intended to start the definition of the strategies to be followed to minimize thermal fluctuations due to the pulsed operation. In particular, the attention has been focussed on the assessment of the DIV CB PHTS temperature behaviour during the pulse-dwell transition so to check the potential effectiveness of a direct coolant temperature control by properly tuning the feedwater mass flow rate.

As already mentioned, the feedwater mass flow rate has been supposed as being given by the sum of two contributions (eq. (1)). Several regulation cases have been investigated by differently weighting the regulation terms as follows:

- Case 1: a PI controller based on the PHTS average temperature regulates the feedwater (W_{PI}=1,W_D=W_t=0);
- Case 2: a PID controller based on the PHTS average temperature regulates the feedwater (W_{PI}=W_D=1, W_t=0);
- Case 3: the feedwater mass flow rate is regulated according to a user-defined function which follows the time trend of thermal power deposited in the in-vessel components (W_{PI}=W_D=0, W_t=1);
- Case 4: the feedwater mass flow rate is given by the sum of the contributions of a user-defined function which follows the time trend of thermal power deposited in the in-vessel components and of a PI controller whose output is dependent on the PHTS average temperature (W_{PI}=W_t=1, W_D=0);
- Case 5: the feedwater mass flow rate is given by the sum of the contributions of a user-defined function which follows the time trend of thermal power deposited in the in-vessel components and of a PID controller whose output is dependent on the PHTS average temperature (W_{PI}=W_t= W_D=1).

Additionally, it has been presumed that the feedwater mass flow rate might be regulated within a range that spans from 5% to 115% of its steady value during the pulse period, which amounts to ≈501 kg/s, while primary pumps are supposed to work at the nominal speed without being regulated so to keep CBs heat transfer capabilities always at their pulse level.

Calculations have included three entire pulse periods with relevant dwell and transition phases to ascertain that the system is able to recover its steady-state pulse conditions, but attention has been mainly focussed on the variation of the main thermal-hydraulic parameters during the pulse-to-dwell transition.

The main results obtained are reported in the following. In particular, figs. 13 and 14 report the trends of feed-water mass flow rate and average temperature, respectively, during the entire simulation and during the pulse to dwell transition. Figs. 15 and 16 describe the coolant temperature during the pulse to dwell transition at the hot and cold leg, i.e. right upstream from the HX and downstream from the pump, respectively.

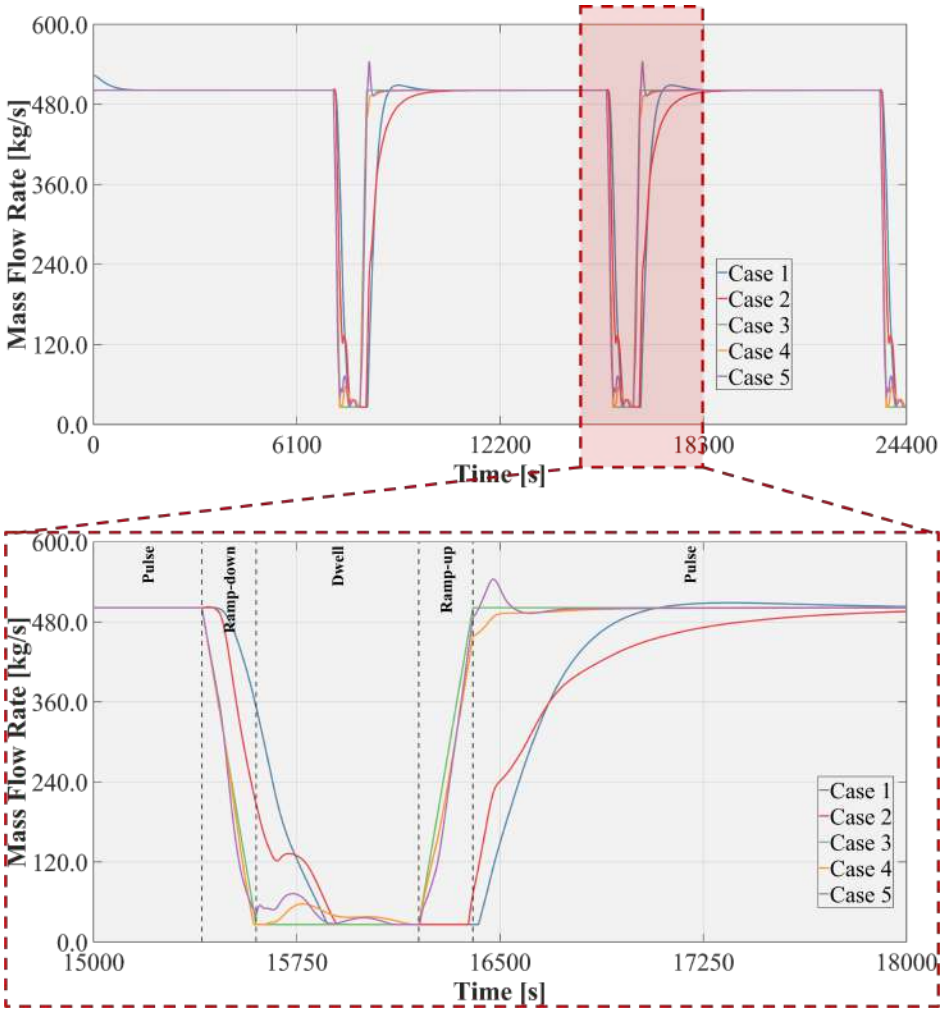

Figure 13: Feed water mass flow rate profile.

Additionally, figs. 17 and 18 show the pressure at the top of the pressurizer and the pressurizer level while table 4 shows a summary comparison of the maximum and minimum values reached by the most relevant thermal-hydraulic quantities in the cases under consideration.

From the analysis of results, it may be argued that the system is not able to quickly recover its nominal pulse conditions in case a PI/PID controller is adopted. In particular, fig. 14 shows that the average temperature takes more than 1000 s to return to its nominal value (i.e. 195°C) after each pulse to dwell transition and maximum variations higher than 3% may be observed both in case a PI or a PID controller is adopted. This reflects on the maximum hot leg temperature which reaches ≈218°C in the former case and ≈217°C in the latter one (see fig. 14).

On the other hand, when considering a user defined regulation based on the expected load variations, the system returns to its nominal pulse conditions in less than 250 s after each pulse to dwell transition and maximum variations in the order of 1% are predicted.

This may be easily explained looking at the considered feedwater control strategies (figs. 13 and 14). The purely automatic control strategies start ramping the feedwater down/up significantly after the beginning of the ramp-down/ramp-up phases because, due to the large system inertia, the average temperature is initially unaffected by the load ramping down/up. This causes the automatic control system to react slowly to load variations. The user defined feedwater control, being synchronised with the anticipated load variations, keeps the average temperature almost constant all over the pulse to dwell transition and the introduction of a PI/PID contribution gives further reactivity to the control systems which may be helpful in coping with unexpected load variations.

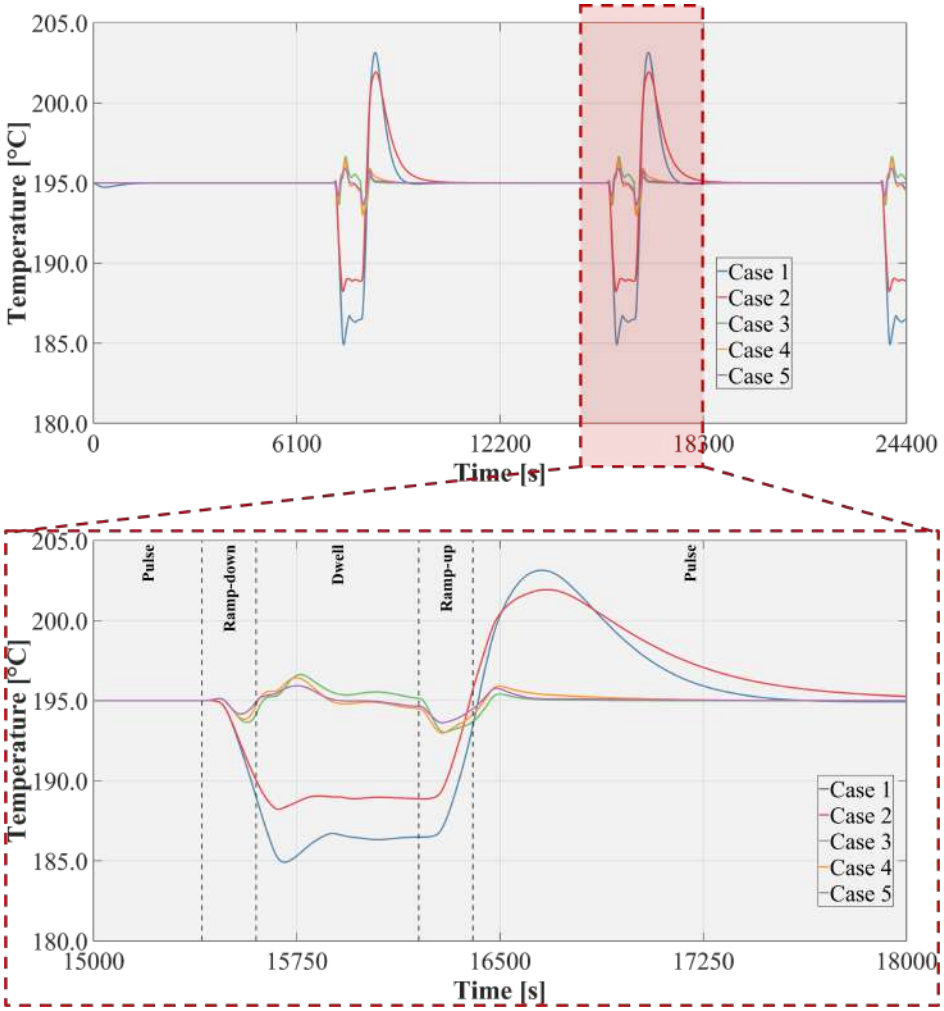

Figure 14: Average temperature profile.

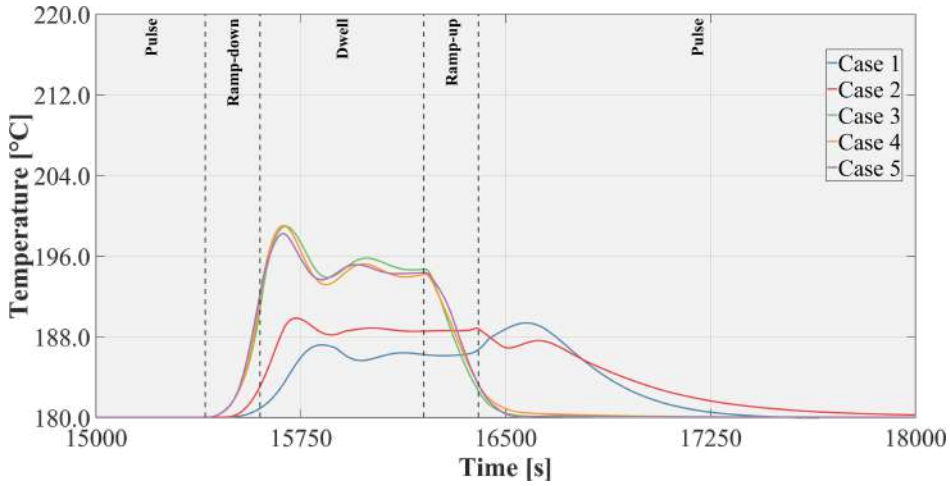

Figure 15: Cold leg temperature during pulse-dwell transition.

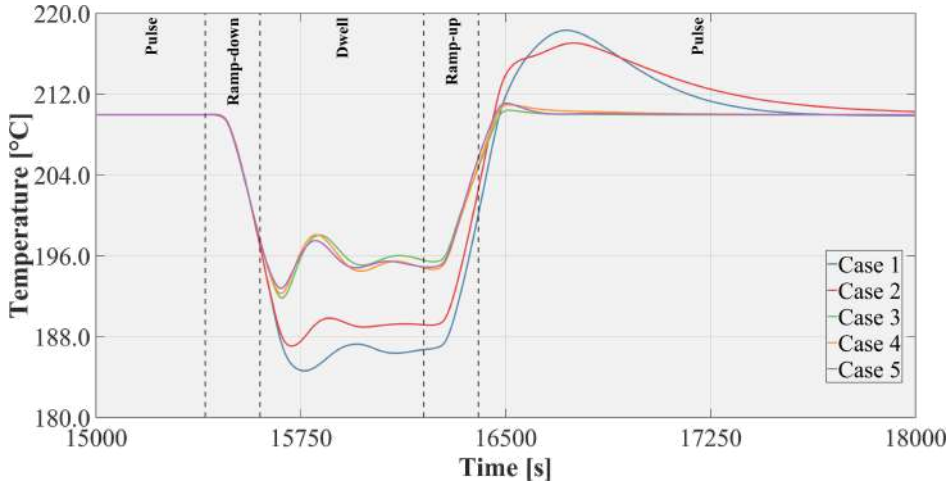

Figure 16: Hot leg temperature during pulse-dwell transition.

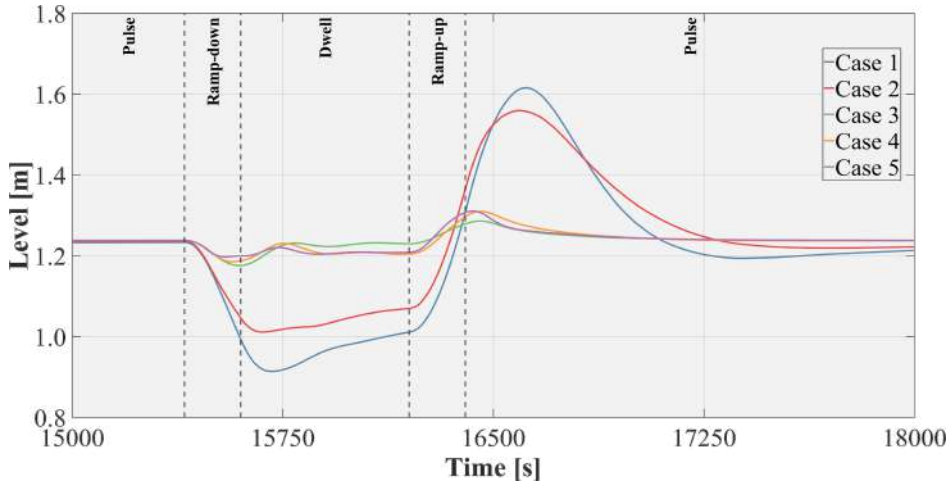

Figure 17: Pressurizer level during pulse-dwell transition.

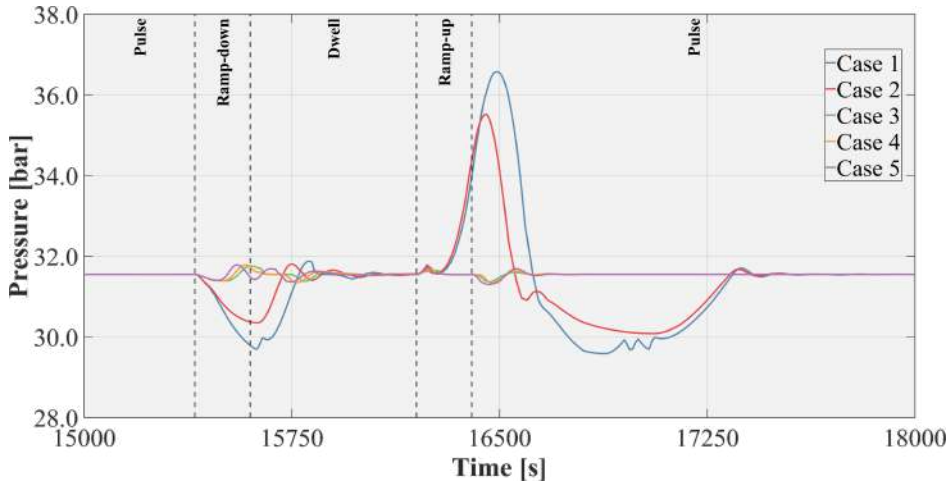

Figure 18: Pressurizer pressure during pulse-dwell transition.

Table 4: Summary comparison of the maximum and minimum thermal-hydraulic parameters.

Parameter	Case 1	Case 2	Case 3	Case 4	Case 5
Target T_{ave} [°C]	195.00	195.00	195.00	195.00	195.00
Min T_{ave} [°C]	184.91	188.22	193.02	192.97	193.63
Max T_{ave} [°C]	203.14	201.93	196.63	196.43	195.93
T_{ave} Max Deviation [-]	-5.18÷4.18%	-3.48÷3.56%	-1.01÷0.84%	-1.04÷0.73%	-0.71÷0.47%
Target $T_{Hot\ Leg}$ [°C]	210.00	210.00	210.00	210.00	210.00
Max $T_{Hot\ Leg}$ [°C]	218.32	217.05	210.40	210.95	211.09
$T_{Hot\ Leg}$ Max Deviation [-]	3.96%	3.36%	0.19%	0.45%	0.52
Target p_{PRZ} [bar]	31.55	31.55	31.55	31.55	31.55
Min p_{PRZ} [bar]	29.59	30.08	31.37	31.32	31.30
Max p_{PRZ} [bar]	36.58	35.54	31.76	31.78	31.79
p_{PRZ} Max Deviation [-]	-6.21÷16.0%	-4.64÷12.6%	-0.56÷0.68%	-0.73÷0.74%	-0.79÷0.75%
Target h_{PRZ} [m]	1.24	1.24	1.24	1.24	1.24
Min h_{PRZ} [m]	0.91	1.01	1.17	1.18	1.20
Max h_{PRZ} [m]	1.62	1.56	1.29	1.31	1.31
h_{PRZ} Max Deviation [-]	-26.0÷30.9%	-18.3÷26.0%	-5.03÷3.97%	-4.24÷5.90%	-3.31÷5.87%

Furthermore, coolant temperature variations cause the coolant to contract or expand thus implying pressure and level variations within the pressurizer. Therefore, the selection of a proper feedwater control strategy would also help in reducing the expected load on the pressurizer during normal operations. In particular, fig. 18 show that large pressure excursions are predicted within the pressurizer in case a purely automatic control strategy is adopted, being in the order of 16% and ≈13% of the nominal PRZ pressure (i.e. 31.55 bar) in case a PI or a PID controller, respectively, is adopted, while, when a user defined regulation based on the expected load variations is considered, the system exhibits much lower pressure variations. Likewise, fig. 17 shows that very large level variations may occur in the first case, being in the order of ±30%, which may be significantly reduced adopting a different control strategy down to values lower than 7%, as confirmed in table 4.

6 Conclusions

Within the framework of the activities promoted by the EUROfusion consortium, a research campaign has been carried out by University of Palermo in cooperation with ENEA to study the thermal-hydraulic behaviour of DIV CB PHTS. The aim of this activity was the assessment of the DIV CB PHTS temperature behaviour during the pulse-dwell transition so to check the potential effectiveness of a direct coolant temperature control by properly tuning the feedwater mass flow rate.

To limit coolant temperature variations within the PHTS, the feedwater mass flow rate has been supposed as being given by the sum of two contributions. The first one is a time profile defined by the user whose trend may be connected to the anticipated load variations, i.e. the ones that may occur during the pulse-dwell transition. The other one is given by a PI or a PID (Proportional-Integral-Differential) controller whose output is dependent on the difference between the actual PHTS average temperature and its target value, i.e. 195 ∘C. Given such a scheme for the control system, several regulation strategies of the feedwater mass flow rate might be envisaged by properly tuning the two contributions and their relative weight. In particular, five cases have been set up with the aim of understanding the potential maximum variations that relevant quantities such as pressure and temperatures can experience for a given Balance of Plant control.

The analyses have highlighted that the system is not able to quickly recover its nominal pulse conditions in case a purely automatic controller is adopted. The purely automatic control strategy starts ramping the feedwater down/up significantly after the beginning of the ramp-down/ramp-up phases because, due to the large system inertia, the average temperature is initially unaffected by the load ramping down/up. This causes the automatic control system to react slowly to load variations. On the other hand, the user defined feedwater control, being synchronised with the anticipated load variations, keeps the average temperature almost constant all over the pulse to dwell transition and the introduction of a PI/PID contribution gives further reactivity to the control systems which may be helpful in coping with unexpected load variations.

Selection of an appropriate feedwater control strategy is essential to allow in-vessel components to always operate at near nominal conditions, mitigating the inevitable cyclic thermal and mechanical stresses that can arise due to pulsed loads. Furthermore, coolant temperature variations cause the coolant to contract or expand thus implying pressure and level variations within the pressurizer. Therefore, it would also help in reducing the expected load on the pressurizer

during normal operations.

CRediT authorship contribution statement

F. M. Castrovinci: Conceptualization, Methodology, Investigation, Writing - original draft. **L. Barucca**: Conceptualization, Methodology, Investigation, Writing - original draft. **R. Burlon**: Conceptualization, Methodology, Investigation, Writing - original draft. **P. Chiovaro**: Conceptualization, Methodology, Investigation, Writing - original draft. **P. A. Di Maio**: Conceptualization, Methodology, Investigation, Writing - original draft. **A. Quartararo**: Conceptualization, Methodology, Investigation, Writing - original draft. **A. Tincani**: Conceptualization, Methodology, Investigation, Writing - original draft. **E. Vallone**: Conceptualization, Methodology, Investigation, Writing - original draft.

Declaration of Competing Interest

The authors declare that they have no known competing financial interests or personal relationships that could have appeared to influence the work reported in this paper.

Acknowledgments

This work has been carried out within the framework of the EUROfusion Consortium, funded by the European Union via the Euratom Research and Training Programme (Grant Agreement No 101052200 — EUROfusion). Views and opinions expressed are however those of the author(s) only and do not necessarily reflect those of the European Union or the European Commission. Neither the European Union nor the European Commission can be held responsible for them.

References

[1] I. Moscato et al. Tokamak cooling systems and power conversion system options. *Fusion Engineering and Design*, 178:113093, 2022.

[2] U.S. Nuclear Regulatory Commission. *TRACE V5.0 THEORY MANUAL*. 2010.

[3] J.H. You et al. Divertor of the European DEMO: Engineering and technologies for power exhaust. *Fusion Engineering and Design*, 175:113010, 2022.

[4] P.A. Di Maio et al. Thermal-hydraulic study of the DEMO divertor cassette body cooling circuit equipped with a liner and two reflector plates. *Fusion Engineering and Design*, 167:112227, 2021.

[5] F. Gillemot et al. *Material Property Handbook pilot project on EUROFER97 (MTA EK, KIT)*. 2016. EUROfusion IDM Ref.: 2MRP77.

[6] *ITER Material Properties Handbook*. ITER Document No. G74 MA 16.

[7] E. Vallone et al. Pre-conceptual design of EU-DEMO divertor primary heat transfer systems. *Fusion Engineering and Design*, 169:112463, 2021.

[8] A. Del Nevo et al. *Direct Coupling of WCLL BB PHTS to PCS feasibility study - Preliminary PCS design with an internal source of energy to operate at a minimum load the steam turbine and the power cycle in dwell*. 2019. EUROfusion IDM Ref.: 2MN55V.

[9] Promat. *MICROTHERM® SLATTED*. Available: https://www.promat.com/en/industry/technologies/microporous/microtherm-slatted/3905/.

[10] ASME. *ASME BPVC - Section II - Subsection D*. ASME, 2015.

[11] Stuart W. Churchill. Friction-factor equation spans all fluid-flow regimes. *Chemical Engineering (New York)*, 84(24):91 – 92, 1977.

[12] F. White. *Fluid Mechanics*. 2008. McGraw-Hill Higher Education.

[13] Salvatore D'Amico et al. Preliminary thermal-hydraulic analysis of the EU-DEMO Helium-Cooled Pebble Bed fusion reactor by using the RELAP5-3D system code. *Fusion Engineering and Design*, 162:112111, 2021.

[14] ANSYS Inc. *ANSYS CFX-Solver Theory Guide*. 2020. Release: 2020 R2.

[15] I. Idelchik. *Handbook of Hydraulic Resistance*. 2008. New Delhi: Jaico Publishing House.

[16] A. Del Nevo et al. *BOP-2.2-T046-D004_WCLL DIV-CAS PHTS DDD (Direct Coupling Option with Small ESS)*. 2020. EUROfusion IDM Ref.: 2NRR9S v1.2.

[17] T. Berry. *Calculation of decay heat in PbLi for entire WCLL reactor*. 2020. EUROfusion IDM Ref.: 2NQL5P.

[18] Stuart W. Churchill and Humbert H.S. Chu. Correlating equations for laminar and turbulent free convection from a horizontal cylinder. *International Journal of Heat and Mass Transfer*, 18(9):1049–1053, 1975.

[19] S. Kakaç, H. Liu and A. Pramuanjaroenkij. *Heat Exchangers Selection, Rating, and Thermal Design*. 2012.

[20] TEMA. *Standards of the Tubular Exchanger Manufacturers Association*. 2007. Tarrytown: Tubular Exchanger Manufacturers Association, Inc.

[21] IAEA. *Pressurized water reactor simulator*. 2005. Workshop Material, Vienna.

[22] Westinghouse. *Westinghouse Technology Systems Manual Section 10.2 Pressurizer Pressure Control System*.

[23] Westinghouse. *Westinghouse Technology Systems Manual Section 10.3 Pressurizer Level Control System*.